QED corrections to radiative recombination and radiative decay of heavy hydrogenlike ions

J. Holmberg,[1] A. N. Artemyev,[2] A. Surzhykov,[3] V. A. Yerokhin,[3,4] and Th. Stöhlker[3,5]
[1]*Physikalisches Institut, Universität Heidelberg, Im Neuenheimer Feld 226, D-69120 Heidelberg, Germany*
[2]*Kassel University, Heinrich Plett Strasse 40, D-34132 Kassel, Germany*
[3]*Helmholtz-Institut Jena, Fröbelstieg 3, D-07743 Jena, Germany*
[4]*Center for Advanced Studies, Peter the Great St. Petersburg Polytechnic University, Polytekhnicheskaya 29, St. Petersburg 195251, Russia*
[5]*Friedrich-Schiller-Universität Jena, Fürstengraben 1, 07743 Jena, Germany*
(Received 20 August 2015; published 14 October 2015)

One-loop quantum electrodynamic (QED) corrections are studied for two basic atomic processes, radiative recombination of an electron with a bare nucleus and radiative decay of a hydrogenlike ion. The perturbations of the bound-state wave function and the binding energy due to the electron self-energy and the vacuum polarization are computed in the Feynman and Coulomb gauges. QED corrections induced by these perturbations are calculated for the differential cross section and the polarization of the emitted radiation in the radiative recombination of an electron and a bare uranium nuclei, as well as the corresponding corrections to the ratio of the $E1$ (electric dipole) and $M2$ (magnetic quadrupole) transition amplitudes in the $2p_{3/2} \to 1s$ radiative decay of hydrogenlike uranium. The results obtained indicate the expected magnitude of the QED effects in these processes on a subpercent level.

DOI: 10.1103/PhysRevA.92.042510 PACS number(s): 31.30.J−, 32.30.−r

I. INTRODUCTION

Radiative recombination of a (quasi-free) electron with a heavy highly charged ion and radiative decay of such ions are basic atomic processes that are extensively studied during the last years in the regime of hard x rays and strong Coulomb fields [1,2]. Radiative recombination, being the time-reversed counterpart of the photoionization, provides an experimental access to this process in the relativistic domain [3,4]. In the case of radiative decay, a precise determination of the ratio of the $E1$ (electric dipole) and the $M2$ (magnetic quadrupole) transition amplitudes and the corresponding transition rates was recently demonstrated [5,6]. The accuracy of these experiments approaches the level at which the influence of QED effects might be discernible.

A complete calculation (even at the one-loop level) of the QED effects in collision processes involving highly charged ions is a very difficult problem. For radiative recombination, no complete calculation has been accomplished so far. The general formulas for this process were derived in Refs. [7,8], but only some corrections were actually calculated. In the case of radiative decay, calculations of the one-loop QED corrections were reported in Ref. [9] for the decay rates of $n = 2$ states of hydrogenlike ions and in Ref. [10] for the fine-structure $M1$ transition amplitudes in boronlike ions.

Recently a formalism for energy-dependent many-body perturbation theory has been developed [11–14] that allows a combined treatment of the QED and electron-correlation effects. While the primary aim of this approach has been the description of QED shifts in energy levels of few-electron atoms, it can be applied to the collision processes as well. In the present work we apply this method to calculations of a set of QED corrections in radiative recombination and radiative decay that are induced by perturbations of the bound-state wave function and the binding energy by the electron self-energy and the vacuum polarization. While such a treatment of QED effects is incomplete at the one-loop level, we believe that the results obtained could be used as an indication of the magnitude of QED effects in the processes considered.

The calculations presented in this work are performed by an extension of the numerical procedure developed in Ref. [15] for the evaluation of the one-loop self-energy correction to the Lamb shift. We extend this procedure to the evaluation of nondiagonal matrix elements of the self-energy operator and compute the radiatively corrected bound-state wave functions and bound-state energies. The resulting energies and wave functions are then used to calculate the differential cross section and the polarization of the emitted radiation in the K-shell radiative recombination of an electron with the initially bare uranium, as well as the ratio of the $M2$ and $E1$ transition amplitudes in the $2p_{3/2} \to 1s$ radiative decay of hydrogenlike uranium.

The outline of the paper is as follows. In Sec. II we describe our numerical method for calculating the matrix elements of the self-energy operator and the perturbations of the wave function induced by the self-energy operator. In Sec. III we briefly discuss the QED corrections to observables in radiative recombination and radiative decay. Section IV is devoted to the presentation and the discussion of our results. Finally, in Sec. V we summarize and provide a brief outlook.

We use units $\hbar = c = 1$ throughout the paper.

II. SELF-ENERGY CORRECTION TO A BOUND-STATE WAVE FUNCTION

The two main QED effects are the self-energy and the vacuum polarization. In this section we will focus on the self-energy since it is the most difficult part to obtain numerically. The vacuum polarization is much simpler to calculate since it is represented by a local radial potential (see, e.g., Refs. [16,17]), which can be included into the Dirac equation or calculated by perturbation theory in a straightforward manner.

A. General background

In the zeroth-order approximation, we start with the relativistic wave functions which are solutions of the Dirac equation with the Coulomb potential describing the nuclear

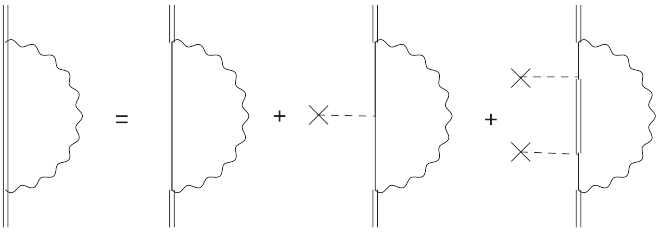

FIG. 1. Expansion of the bound electron self-energy in terms of scattering order with the nuclear Coulomb potential. The double lines denote electrons propagating in the presence of the potential and the single lines denote freely propagating electrons. The wavy lines denote virtual photons.

binding field,

$$[\boldsymbol{\alpha}\cdot\boldsymbol{p}+\beta m+V_{\rm nuc}(\mathbf{r})-E]\,\Phi(\mathbf{r})=0, \tag{1}$$

where $\boldsymbol{\alpha}$ and β are the Dirac matrices, $V_{\rm nuc}$ is the nuclear potential, and m and E are the electron mass and energy, respectively. The solutions of this equation are of the form

$$\Phi_{n,\kappa,m}(\mathbf{r})=\frac{1}{r}\begin{pmatrix}F_{n,\kappa}(r)\chi^{m}_{\kappa}(\theta,\varphi)\\ iG_{n,\kappa}(r)\chi^{m}_{-\kappa}(\theta,\varphi)\end{pmatrix}, \tag{2}$$

where F and G are known as the large and small radial components, respectively, χ is an ls-coupled spherical spinor, n is the principal quantum number, and κ is Dirac's angular-momentum quantum number $\kappa=(-1)^{j+l+\frac{1}{2}}(j+\frac{1}{2})$ determined by the orbital angular momentum l and the total angular momentum j. The projection of j is given by m.

In this section we will be interested in the corrections to the Dirac wave functions (2) arising from the electron self-interaction as predicted by QED. In order to simplify further expressions, we introduce a collective index t such that $\Phi_{n,\kappa,m}\equiv\Phi_t$ and let $|t\rangle$ denote the state vector which corresponds to Φ_t. Furthermore, we reserve the index a for the state whose corrections we wish to study (the *model state*). The correction to the model state due to the first-order self-energy can then be written as

$$|\delta a^{\rm SE}\rangle=\sum_{t\neq a}\frac{|t\rangle\langle t|\Sigma^{\rm ren}_{\rm B}(E_a)|a\rangle}{E_a-E_t}, \tag{3}$$

where $\Sigma^{\rm ren}_{\rm B}=\Sigma_{\rm B}-\delta m$ is the renormalized bound[1] electron self-energy operator.

The evaluation of the matrix elements of the operator $\Sigma^{\rm ren}_{\rm B}$ has been extensively studied in the literature and different approaches have been developed to tackle this problem [18–26]. In our work we use the method originally proposed by Brown *et al.* [27] and further developed by Blundell and Snyderman [20]. This method expands the unrenormalized operator $\Sigma_{\rm B}$ in terms of scattering order with the nuclear potential (see Fig. 1). The terms of this expansion are renormalized and the matrix elements of $\Sigma^{\rm ren}_{\rm B}$ are obtained as the sum of a zero-potential, a one-potential, and a many-potential term:

$$\langle t|\Sigma^{\rm ren}_{\rm B}|a\rangle=\Sigma^{\rm ZP}_{ta}+\Sigma^{\rm OP}_{ta}+\Sigma^{\rm MP}_{ta}, \tag{4}$$

where

$$\Sigma^{\rm ZP}_{ta}=\langle t|\Sigma^{\rm ren}_{\rm free}|a\rangle \tag{5}$$

is the matrix element of the renormalized free-electron self-energy operator $\Sigma^{\rm ren}_{\rm free}$ and

$$\Sigma^{\rm OP}_{ta}=\langle t|\Lambda^{0,{\rm ren}}_{\rm free}V_{\rm nuc}|a\rangle, \tag{6}$$

where $\Lambda^{0,{\rm ren}}_{\rm free}$ is the (scalar part of the) renormalized free-electron vertex operator. The remaining many-potential term can be formulated by using the Feynman rules of bound-state QED, see, e.g., Ref. [20].

The first-order perturbation of the the model-state wave function $|a\rangle$ by the electron self-energy can thus be written as

$$\begin{aligned}|\delta a^{\rm SE}\rangle&=\sum_{t\neq a}\frac{|t\rangle\langle t|\Sigma^{\rm ren}_{\rm B}|a\rangle}{E_a-E_t}\\&=\sum_{t\neq a}\frac{|t\rangle\left(\Sigma^{\rm ZP}_{ta}+\Sigma^{\rm OP}_{ta}+\Sigma^{\rm MP}_{ta}\right)}{E_a-E_t}\\&\equiv|\delta a^{\rm ZP}\rangle+|\delta a^{\rm OP}\rangle+|\delta a^{\rm MP}\rangle.\end{aligned} \tag{7}$$

The matrix elements in Eq. (7) are nonzero only if $|a\rangle$ and $|t\rangle$ have the same spin-angular dependence ($\kappa_a=\kappa_t$ and $m_a=m_t$), which means that the self-energy affects only the radial part of the wave function.

We now proceed to discuss how the three corrections in (7) can be computed. The many-potential term and the perturbation of the wave function involve summations over the spectrum of the Dirac equation. For computing such sums, we use the method of space discretization [28,29]. The complete numerical spectrum is obtained by solving the Dirac equation (1) for each κ on a discretized radial grid. This allows for a straightforward inclusion of the finite-nucleus effect using essentially arbitrary (spherically symmetric) nuclear models. The r variable is confined to the interval $0<r<R$, where R is chosen large enough that its particular choice does not influence the final results. A series of calculations are performed on r grids of increasing resolution and the continuum limit can be found by extrapolation.

B. Zero- and one-potential terms

The zero- and one-potential terms are given by the matrix elements of the renormalized free-electron self-energy and vertex-correction operators, respectively [Eqs. (5) and (6)]. These operators are most easily constructed in momentum space using dimensional regularization (see Refs. [30–32] for details). The resulting matrix elements can in principle be calculated with respect to the momentum distributions of the states $|a\rangle$ and $|t\rangle$.

However, although $\langle\mathbf{p}|a\rangle$ can be rather easily calculated for the lowest-lying bound states, it is numerically difficult to obtain $\langle\mathbf{p}|t\rangle$ to sufficient accuracy for highly excited discretized states $|t\rangle$. These states acquire contributions from a wide range of momenta, and their numerical Fourier transform can introduce large numerical errors.

[1]For brevity we refer to operators containing electrons propagating in the nuclear potential as bound operators, although the propagating electrons may have arbitrarily high energies. This is to distinguish these operators from those containing freely propagating electrons.

It is more convenient to work directly with the function defined by the sum over states in Eq. (3) (the *restricted* radial Green's function):

$$G_\kappa^a(r,r',E_a) = \sum_{t\neq a} \frac{\langle r|t\rangle\langle t|r'\rangle}{E_a - E_t} = \sum_{t\neq a} \frac{\Phi_t(r)\Phi_t^\dagger(r')}{E_a - E_t}. \quad (8)$$

This function is localized and its discretized form is reasonably smooth in both coordinates. Its Fourier transform with respect to r' is given by

$$G_\kappa^a(r,p,E_a) = \sqrt{\frac{2}{\pi}} \int dr'\, r'^2 (-i)^l j_l(pr') \sum_{t\neq a} \frac{\Phi_t(r)\Phi_t^\dagger(r')}{E_a - E_t}, \quad (9)$$

where the index l of the spherical Bessel function j_l depends upon which component (large or small) of $\Phi_t^\dagger(r')$ is considered. This transform can be computed numerically without too much difficulty.

Having obtained $G_\kappa^a(r,p,E_a)$ from Eq. (9), we can get the radial representations of the zero- and one-potential self-energy corrections to the wave function as

$$\langle r|\delta a^{\rm ZP}\rangle = \int dp\, p^2 G_\kappa^a(r,p,E_a)\Sigma_{\rm free}^{\rm ren}(p,E_a)\Phi_a(p) \quad (10)$$

and

$$\langle r|\delta a^{\rm OP}\rangle = \int dp p^2 \int dp'\, p'^2 \int_{-1}^{1} d(\cos\vartheta) G_\kappa^a(r,p,E_a) \times \Lambda_{\rm free}^{0,{\rm ren}}(p,p',\vartheta,E_a) V_{\rm nuc}(k)\Phi_a(p'), \quad (11)$$

where ϑ is the angle between $\mathbf{p}$ and $\mathbf{p}'$ and $k = |\mathbf{p} - \mathbf{p}'|$. Here $\Phi_a(p)$ is the momentum distribution of $|a\rangle$ which can be obtained similarly to Eq. (9).

The Fourier transformations are performed by interpolating the integrand to continuous space using Lagrange polynomials. The integration between grid points can then be treated semianalytically using recursion relations for integrals of the combinations $j_l(pr)\, r^m$ of spherical Bessel functions and powers of r that appear.

Expressions for the momentum-space matrix elements (5) and (6) were presented in Feynman gauge in Ref. [30] and in Coulomb gauge in Ref. [15]. Note that the expressions for the free vertex operator $\Lambda_{\rm free}^{0,{\rm ren}}$ given in these references are valid only for the diagonal matrix elements and must be modified to account for the fact that the integrand is not symmetric with respect to $p \leftrightarrow p'$ in the general case.

C. Many-potential term

By using the Feynman diagram technique of bound-state QED, the many-potential term can be written in coordinate space as a sum over the orbital angular momentum l of the virtual photon:

$$\Sigma_{ta}^{\rm MP} = \sum_{l=0}^{\infty} \Sigma_{ta}^{{\rm MP},l}. \quad (12)$$

Each term in this sum can be calculated using the expansion of the self-energy operator (Fig. 1) as

$$\Sigma_{ta}^{{\rm MP},l} = \langle t|\Sigma_{\rm B}|a\rangle^l - \langle t|\Sigma_{\rm free}|a\rangle^l - \langle t|\Lambda_{\rm free}^0 V_{\rm nuc}|a\rangle^l. \quad (13)$$

Here all operators on the right-hand side are unrenormalized and constructed in coordinate space. After the subtraction (13) is performed for a fixed l, the summation (12) becomes convergent and can be evaluated numerically. In actual calculations, the sum over l is necessarily truncated and should be in principle extrapolated to infinity. However, we have found that using a fixed truncation limit at $l = 50$ introduces a relative error in the many-potential part of the wave function correction of less than 0.05% for $Z = 92$.

The Feynman-gauge expression for the many-potential term is given by

$$\Sigma_{ta}^{{\rm MP},l} = -\frac{\alpha}{\pi}(2l+1)\int k\, dk \left\{ \sum_m \frac{\langle t|\alpha^\mu j_l(kr_1)\mathbf{C}^l|m\rangle\langle m|j_l(kr_2)\mathbf{C}^l\alpha_\mu|a\rangle}{E_a - E_m - {\rm sign}(E_m)k} - \sum_p \frac{\langle t|\alpha^\mu j_l(kr_1)\mathbf{C}^l|p\rangle\langle p|j_l(kr_2)\mathbf{C}^l\alpha_\mu|a\rangle}{E_a - E_p - {\rm sign}(E_p)k} - \sum_{p,q} \frac{\langle t|\alpha^\mu j_l(kr_1)\mathbf{C}^l|p\rangle\langle p|V_{\rm nuc}|q\rangle\langle q|j_l(kr_2)\mathbf{C}^l\alpha_\mu|a\rangle}{[E_a - E_p - {\rm sign}(E_p)k][E_a - E_q - {\rm sign}(E_q)k]} F \right\}. \quad (14)$$

Here the states $|m\rangle$ are generated in the nuclear potential and $|p\rangle$ and $|q\rangle$ refer to states generated in the limit $Z \to 0$. The $\mathbf{C}^l$ are spherical tensors whose components are related to the spherical harmonics Y_m^l by

$$C_m^l(\theta,\phi) = \sqrt{\frac{4\pi}{(2l+1)}}\, Y_m^l(\theta,\phi). \quad (15)$$

The function F is given by

$$F = 1 + [{\rm sign}(E_p) - {\rm sign}(E_q)]\frac{k}{E_p - E_q} \quad (16)$$

and ensures proper treatment of negative-energy states in the third term (the "vertex" term). The corresponding expression for $\Sigma_{ta}^{{\rm MP},l}$ in Coulomb gauge can be found in Ref. [15].

The first term on the right-hand side of Eq. (14) (the "bound" term) contains a pole on the k axis whenever there is an intermediate state $|m_0\rangle$ with a positive energy $E_{m_0} < E_a$. This situation can appear if $|a\rangle$ is not the ground state, and the appearance of the pole is related to the spontaneous decay of the excited state. In this case one has to perform a numerical Cauchy principal-value (CPV) integral over k when evaluating Eq. (14).

In order to accomplish the CPV integration in a numerically stable way, we first note that the integrand of the bound term

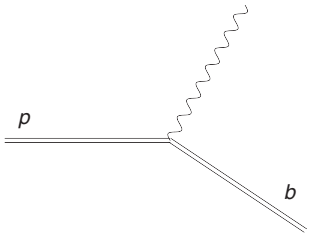

FIG. 2. Feynman diagram for the radiative recombination process in the leading-order approximation. The continuum electron is denoted by p and the bound atomic electron is denoted by b.

for the intermediate pole-state $|m_0\rangle$ is of the form

$$f(k) = \frac{g(k)}{\omega_0 - k}, \tag{17}$$

where the pole is located at $\omega_0 = E_a - E_{m_0}$. Next we separate out the singular part:

$$f(k) = f(k) - \frac{g(\omega_0)}{\omega_0 - k} + \frac{g(\omega_0)}{\omega_0 - k} \equiv h(k) + \frac{g(\omega_0)}{\omega_0 - k}, \tag{18}$$

where now

$$h(k) = \frac{g(k) - g(\omega_0)}{\omega_0 - k} \tag{19}$$

contains no poles and can be integrated numerically without difficulty. The CPV integral of the remaining term can be evaluated analytically over a suitable interval $[0,C]$ that includes ω_0 to give

$$\int_0^C dk \frac{g(\omega_0)}{\omega_0 - k} = -g(\omega_0) \ln\left(\left|1 - \frac{C}{\omega_0}\right|\right). \tag{20}$$

The total integral thus becomes

$$\int_0^\infty dk f(k) = -g(\omega_0) \ln\left(\left|1 - \frac{C}{\omega_0}\right|\right) + \int_0^C dk h(k) + \int_C^\infty dk f(k). \tag{21}$$

Having obtained the self-energy correction to the wave function, we now proceed to describe two applications.

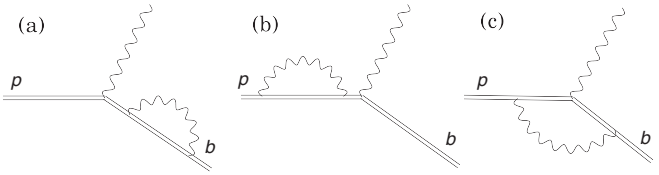

FIG. 3. Feynman diagrams for the one-loop self-energy corrections to the radiative recombination process.

III. CALCULATION OF AMPLITUDES FOR ATOMIC PROCESSES

A straightforward application of our QED-corrected wave functions is to compute corrections to observables in basic atomic processes. We will here consider two such processes in hydrogenlike uranium, namely radiative recombination of an electron into the K shell, as well as the $2p_{3/2} \to 1s$ radiative decay. We begin with radiative recombination.

A. Radiative recombination

Radiative recombination is the process in which a charged ion captures an electron from the continuum with the emission of a photon. The observable properties of this process can be traced back to the corresponding transition amplitude τ. In zeroth order, the amplitude of the capture of the continuum electron with asymptotic four-momentum p, spin projection μ, and charge $-e$ into the bound state $|a\rangle$ of an initially bare atomic nucleus is given by [8,33]

$$\tau^{(0)} = -e\langle a|\alpha^\nu A^*_\nu(\mathbf{k},\mathbf{x})|p,\mu\rangle, \tag{22}$$

where

$$A^\nu(\mathbf{k},\mathbf{x}) = \frac{\epsilon^\nu e^{i\mathbf{k}\cdot\mathbf{x}}}{\sqrt{2\omega(2\pi)^3}} \tag{23}$$

is the four-potential of the emitted photon with wave vector $\mathbf{k}$, energy $\omega = |\mathbf{k}|$, and polarization vector ϵ^ν. The Feynman diagram for this amplitude is shown in Fig. 2.

General expressions for the one-loop QED corrections to this amplitude were derived in Refs. [8,34]; the corresponding Feynman diagrams are shown in Figs. 3 and 4. The contributions from the electron self-energy (Fig. 3) are

$$\tau^{(1)}_{\mathrm{SE}} = -\left[\sum_{t\neq a} \frac{\langle a|\Sigma^{\mathrm{ren}}_{\mathrm{B}}(E_a)|t\rangle\langle t|e\alpha^\nu A^*_\nu|p,\mu\rangle}{E_a - E_t} + \frac{1}{2}\langle a|\frac{\partial\Sigma_{\mathrm{B}}}{\partial E}|a\rangle\langle a|e\alpha^\nu A^*_\nu|p,\mu\rangle + \sum_t \frac{\langle a|e\alpha^\nu A^*_\nu|t\rangle\langle t|\Sigma^{\mathrm{ren}}_{\mathrm{B}}(p^0)|p,\mu\rangle}{p^0 - E_t(1-i\varepsilon)} + \int d\mathbf{z} e A^*_\nu(\mathbf{z})\Lambda^\nu_{\mathrm{B}}(E_a,p^0,\mathbf{z}) + \left(Z_2^{-1/2} - 1\right)\langle a|e\alpha^\nu A^*_\nu|p,\mu\rangle\right], \tag{24}$$

where Λ^ν_{B} is the bound vertex-correction operator and Z_2 is a renormalization constant. The corresponding vacuum-polarization corrections are (Fig. 4)

$$\tau^{(1)}_{\mathrm{VP}} = -\left[\sum_{t\neq a} \frac{\langle a|U_{\mathrm{VP}}|t\rangle\langle t|e\alpha^\nu A^*_\nu|p,\mu\rangle}{E_a - E_t} + \sum_t \frac{\langle a|e\alpha^\nu A^*_\nu|t\rangle\langle t|U_{\mathrm{VP}}|p,\mu\rangle}{p^0 - E_t(1-i\varepsilon)} + \int d\mathbf{z}\int d\mathbf{x}\int d\mathbf{y} e A^*_\nu(\mathbf{z})\psi^\dagger_a(\mathbf{x})\alpha^\lambda\psi_{p,\mu}(\mathbf{x})D_{\lambda\sigma}(\omega,\mathbf{x}-\mathbf{y})\Pi^{\sigma\nu}(\omega,\mathbf{y},\mathbf{z}) + \left(Z_3^{-1/2} - 1\right)\langle a|e\alpha^\nu A^*_\nu|p,\mu\rangle\right], \tag{25}$$

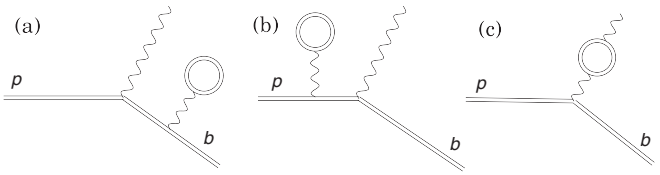

FIG. 4. Feynman diagrams for the one-loop vacuum-polarization corrections to the radiative recombination process.

where $U_{\rm VP}$ is the vacuum-polarization potential, $D_{\lambda\sigma}$ is the photon propagator, $\Pi^{\sigma\nu}$ is the polarization tensor for the photon self-energy, and Z_3 is a renormalization constant.

The first term on the right-hand side of Eq. (24) is just [see Eq. (3)]

$$\sum_{t\neq a}\frac{\langle a|\Sigma_{\rm B}^{\rm ren}(E_a)|t\rangle\langle t|e\alpha^\nu A^*_\nu|p,\mu\rangle}{E_a-E_t}=\langle\delta a^{\rm SE}|e\alpha^\nu A^*_\nu|p,\mu\rangle, \tag{26}$$

which means that it can be computed with the self-energy corrected wave function $|\delta a^{\rm SE}\rangle$ by making the substitution $\langle a|\to\langle\delta a^{\rm SE}|$ in Eq. (22). The corresponding term in the vacuum-polarization corrections can be treated similarly by the substitution $\langle a|\to\langle\delta a^{\rm VP}|$ with the VP-corrected wave function

$$|\delta a^{\rm VP}\rangle=\sum_{t\neq a}\frac{|t\rangle\langle t|U_{\rm VP}(r)|a\rangle}{E_a-E_t}. \tag{27}$$

The dominant contribution to $U_{\rm VP}(r)$ is given by the Uehling potential, which corresponds to considering only freely propagating fermions interacting once with the nuclear potential inside the fermion loops. The remaining Wichmann-Kroll contribution is more difficult to evaluate, but can be computed to very good accuracy using the approximate formulas in Ref. [35].

In the present work we calculate only the first terms in the right-hand side of Eqs. (24) and (25), which correspond to the diagrams in Figs. 3(a) and 4(a). In the case of vacuum polarization, the diagram 4(b) can be easily evaluated as well. However, its contribution is expected [8] to be largely canceled by the corresponding self-energy diagram, so we do not include it into our calculation. The remaining vacuum-polarization contribution should be small, as it vanishes in the Uehling approximation. The omitted self-energy terms in Eq. (24) are generally not small. At present we are not able to calculate them; such calculation would require development of new computational methods.

Let us now briefly describe how to obtain corrections to observable quantities from the transition amplitude. The differential cross section for the emission of a photon with energy $\omega=|\mathbf{k}|$ into the solid-angle element $d\Omega$ is connected to the transition amplitude τ by the expression [8]

$$\frac{d\sigma}{d\Omega}=\frac{(2\pi)^4}{|\mathbf{v}|}\mathbf{k}^2\tau^*\tau, \tag{28}$$

where $\mathbf{v}$ is the velocity of the initial continuum electron with respect to the ion. The transition amplitude can be expanded in terms of the fine-structure constant α,

$$\tau=\tau^{(0)}+\tau^{(1)}+\cdots, \tag{29}$$

yielding the zeroth-order differential cross section as

$$\frac{d\sigma^{(0)}}{d\Omega}=\frac{(2\pi)^4}{|\mathbf{v}|}\mathbf{k}^2\tau^{(0)*}\tau^{(0)}. \tag{30}$$

The first-order (in α) correction to the cross section is induced by the correction to the transition amplitude $\tau^{(1)}$ and by the shift of the energy of the emitted photon,

$$\frac{d\sigma^{(1)}}{d\Omega}=\frac{(2\pi)^4}{|\mathbf{v}|}\mathbf{k}^2(\tau^{(0)*}\tau^{(1)}+\tau^{(1)*}\tau^{(0)})+\frac{d\sigma^{(0)}}{d\Omega}\bigg|_{\omega=p^0-E_a^{\rm QED,(1)}}-\frac{d\sigma^{(0)}}{d\Omega}\bigg|_{\omega=p^0-E_a}, \tag{31}$$

where $E_a^{\rm QED,(1)}$ is the energy of the state a corrected by the one-loop QED effects and E_a is the energy of this state without QED effects. The self-energy and vacuum-polarization contributions to $\tau^{(1)}$ are given by Eqs. (24) and (25).

Apart from corrections to the cross section, we wish also to study the QED effects on the linear polarization of the radiation emitted in the process. In order to describe the polarization we make use of the Stokes parameters P_1, P_2, and P_3. The first Stokes parameter P_1 can be accessed in experiment as

$$P_1=\frac{I_{0^\circ}-I_{90^\circ}}{I_{0^\circ}+I_{90^\circ}}, \tag{32}$$

where I_x is the intensity of radiation whose linear polarization vector makes an angle of x degrees relative to the reaction plane. The reaction plane is defined as the plane spanned by the momentum vector $\mathbf{p}$ of the incoming continuum electron and the wave vector $\mathbf{k}$ of the emitted photon. P_1 ranges from -1 (the polarization completely perpendicular to the reaction plane) to $+1$ (the polarization completely parallel to the reaction plane). P_2 can be constructed similarly to P_1 but intensities should be taken at angles of $x=45^\circ$ and $x=135^\circ$. As discussed in Ref. [33], P_2 in radiative recombination is proportional to the degree of spin polarization of the incoming continuum electrons. In the present paper we assume the initial-state electrons to be unpolarized, so that P_2 vanishes. The third Stokes parameter P_3 corresponds to the degree of circular polarization and will not be considered here.

In order to compute P_1 we express it in terms of the differential cross sections for two polarizations of the emitted radiation: one with the polarization parallel to the reaction plane $(d\sigma/d\Omega)_\parallel$, and another with the polarization perpendicular to this plane $(d\sigma/d\Omega)_\perp$. The resulting Stokes parameter P_1 is then obtained as

$$P_1=\frac{\left(\frac{d\sigma}{d\Omega}\right)_\parallel-\left(\frac{d\sigma}{d\Omega}\right)_\perp}{\left(\frac{d\sigma}{d\Omega}\right)_\parallel+\left(\frac{d\sigma}{d\Omega}\right)_\perp}. \tag{33}$$

QED effects modifying the cross section $d\sigma/d\Omega$ induce the corresponding corrections to P_1. In this work we will study the QED correction to P_1 defined as the difference of P_1 computed with including the QED effects and without them,

$$\delta P_1=P_1(\text{with QED})-P_1(\text{without QED}). \tag{34}$$

B. Radiative decay

As a second application of our radiatively corrected wave functions we consider the $2p_{3/2}\to 1s$ radiative decay in

hydrogenlike uranium. Because of the angular momentum and parity selection rules, this decay can proceed both via the $E1$ (electric dipole) and $M2$ (magnetic quadrupole) channels. It was recently shown [5] that it is possible to gain direct experimental access to the ratio τ_{M2}/τ_{E1} of the corresponding transition amplitudes. We will here consider one-loop QED corrections to this ratio.

The separation of the radiative decay into different channels is a consequence of the expansion of the radiation field into so-called multipole components. We will here just briefly recall how this expansion is defined; for further details we refer to Ref. [36].

The spatial part of the four-potential (23) can be written as (for a particular photon helicity $\lambda = \pm 1$)

$$\begin{aligned}\mathbf{A}_\lambda(\mathbf{k},\mathbf{r}) =& \frac{\boldsymbol{\epsilon}_\lambda e^{i\mathbf{k}\cdot\mathbf{r}}}{\sqrt{2\omega(2\pi)^3}} \\ =& \frac{1}{\sqrt{2\omega(2\pi)^2}} \sum_{L=0}^{\infty} \sum_{M=-L}^{L} i^L \sqrt{2L+1} \\ & \times D^L_{M\lambda}(\mathbf{z}\to\mathbf{k}) \big[\mathbf{A}^M_L(m) + i\lambda \mathbf{A}^M_L(e)\big], \end{aligned} \tag{35}$$

where, in the Coulomb gauge,

$$\mathbf{A}^M_L(m) = j_L(|\mathbf{k}|r)\mathbf{T}^M_{L,L} \tag{36}$$

is the magnetic component and

$$\begin{aligned}\mathbf{A}^M_L(e) =& \sqrt{\frac{L+1}{2L+1}}\, j_{L-1}(|\mathbf{k}|r)\mathbf{T}^M_{L,L-1} \\ & - \sqrt{\frac{L}{2L+1}}\, j_{L+1}(|\mathbf{k}|r)\mathbf{T}^M_{L,L+1} \end{aligned} \tag{37}$$

is the electric component, both defined in terms of the so-called vector spherical harmonics $\mathbf{T}^M_{L,L'}$. In Eq. (35) $D^L_{M\lambda}(\mathbf{z}\to\mathbf{k})$ is the Wigner rotation matrix which rotates the radiation field from the quantization axis $\mathbf{z}$ into the actual propagation direction $\mathbf{k}$. The magnetic quadrupole and electric dipole components of the radiation field are given by Eq. (36) with $L = 2$, and Eq. (37) with $L = 1$, respectively.

The zeroth-order transition amplitudes of the $E1$ and $M2$ transitions are proportional to the reduced matrix elements of the corresponding multipole components,

$$\begin{aligned}\tau^{(0)}_{E1} &= C\,\langle a||\boldsymbol{\alpha}\cdot\mathbf{A}_1(e)||b\rangle, \\ \tau^{(0)}_{M2} &= C\,\langle a||\boldsymbol{\alpha}\cdot\mathbf{A}_2(m)||b\rangle, \end{aligned} \tag{38}$$

where $|a\rangle$ is the $1s$ state and $|b\rangle$ is the $2p_{3/2}$ state. The energy of the emitted photon is given by $\omega = |\mathbf{k}| = E_b - E_a$. C is some overall prefactor which is not relevant for the present work as it cancels in the ratio $\tau^{(0)}_{E1}/\tau^{(0)}_{M2}$.

The QED corrections to the $E1$ amplitude due to perturbations of the wave functions and due to the shift of the transition energy can be expressed as

$$\begin{aligned}\tau^{(1)}_{E1} =& C\,\langle \delta a^{\rm SE}||\boldsymbol{\alpha}\cdot\mathbf{A}_1(e)||b\rangle + \langle a||\boldsymbol{\alpha}\cdot\mathbf{A}_1(e)||\delta b^{\rm SE}\rangle \\ & + C\,\langle \delta a^{\rm VP}||\boldsymbol{\alpha}\cdot\mathbf{A}_1(e)||b\rangle + \langle a||\boldsymbol{\alpha}\cdot\mathbf{A}_1(e)||\delta b^{\rm VP}\rangle \\ & + \tau^{(0)}_{E1}\Big|_{\omega=E_a^{\rm QED,(1)}-E_b^{\rm QED,(1)}} - \tau^{(0)}_{E1}\Big|_{\omega=E_a-E_b}, \end{aligned} \tag{39}$$

and the same for $\tau^{(1)}_{M2}$.

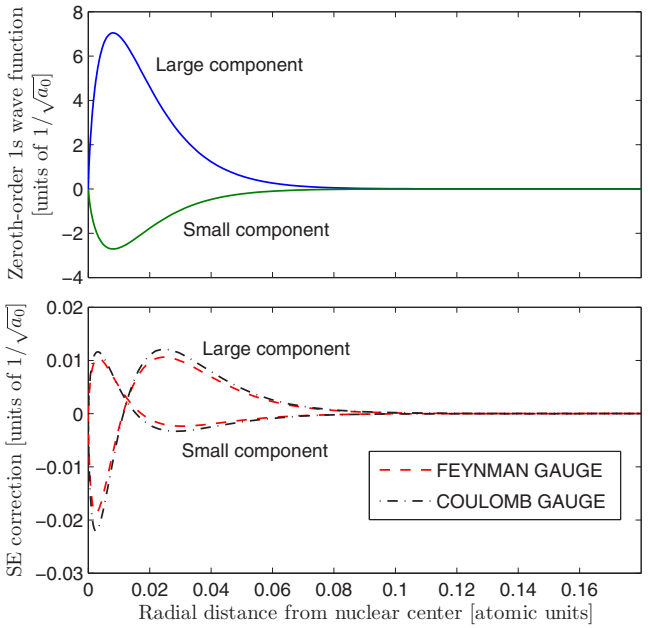

FIG. 5. (Color online) The zeroth-order radial wave function of the $1s$ state (top) and the self-energy (SE) correction in Feynman gauge and Coulomb gauge (bottom) for $Z = 92$. The correction shifts the wave function outward radially which corresponds to a less strongly bound electron. The radial unit is the Bohr radius a_0 and the wave functions are given in units of $1/\sqrt{a_0}$.

Similarly to the radiative recombination case, the correction (39) represent only a part of the total one-loop QED effect. Further corrections containing the so-called vertex contributions [diagram in Fig. 3(c)] and terms with the

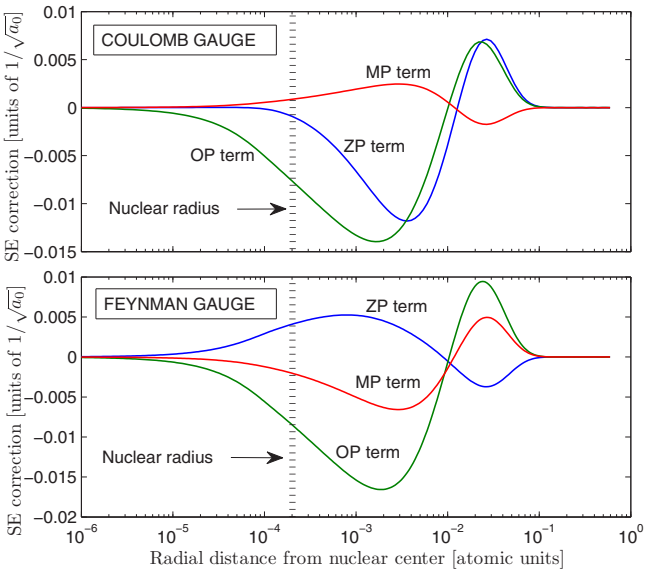

FIG. 6. (Color online) A comparison of the contributions from the different terms in expansion (7) of the total self-energy correction to the large component of the $1s$ wave function for $Z = 92$, as calculated in the Feynman and Coulomb gauges. The x axis is logarithmic in order to enhance the nuclear region. Units are the same as in Fig. 5.

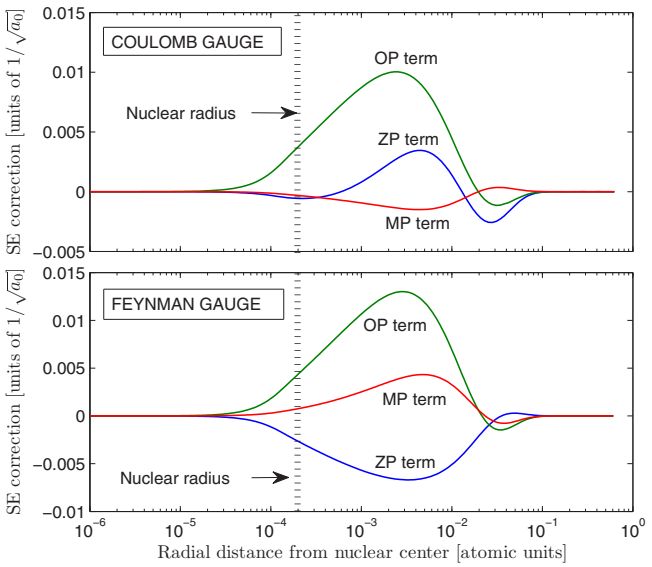

FIG. 7. (Color online) Same as Fig. 6 but for the small component.

derivative of the self-energy operator [9,10] are not calculated here.

IV. RESULTS AND DISCUSSION

A. Self-energy correction to the atomic wave function

The electron self-energy effects has been intensively studied in the past in the context of the binding energy, the hyperfine splitting, the bound-electron g factor, etc. The corresponding corrections to the wave function, however, received much less attention so far. Although the wave functions themselves are unobservable, it might nevertheless be instructive to see how they are affected by the inclusion of QED effects. This may help to gain intuition for how these effects influence various physical properties and processes.

In Fig. 5 we plot the self-energy correction to the radial wave function $|\delta a^{\rm SE}\rangle$ for the $1s$ state in hydrogenlike uranium as computed in Feynman and Coulomb gauge. Our calculations are performed for the homogeneous nuclear charge distribution with radius $R_{\rm nuc} = 5.863$ fm. Note that the self-energy correction shifts the wave function outward radially, which corresponds to a less strongly bound electron. This is in agreement with the positive sign of the associated energy shift (see, e.g., Ref. [15]). As expected, the wave function correction is not gauge invariant. The gauge invariance will be recovered for observable quantities when all corrections of the given order of α are combined together. Nevertheless, the difference between the corrections in the two gauges is quite small and both corrections display very similar radial behavior.

Figures 6 and 7 display the semi-log plots which compare the contributions of the three terms in Eq. (7) to the total self-energy wave-function correction in the two gauges, for the large and small components. It is interesting that the one-potential term is roughly the same in both gauges, whereas the zero-potential and many-potential terms play opposite roles in Coulomb and Feynman gauge. Furthermore, in Coulomb

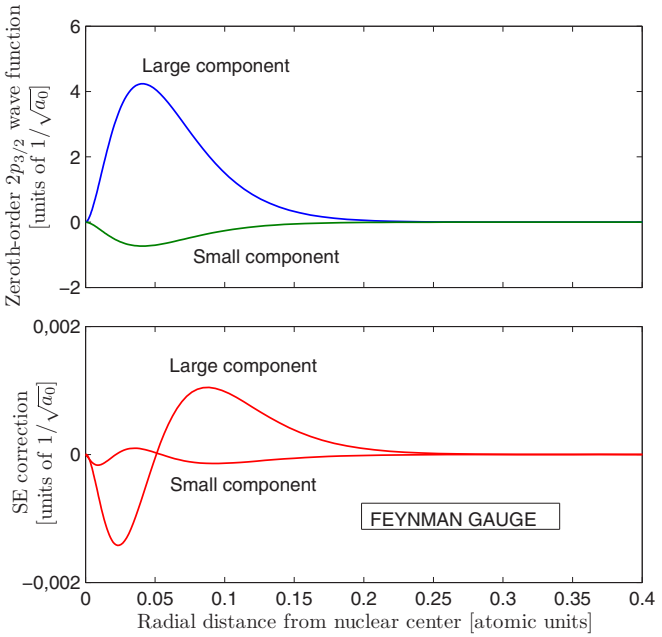

FIG. 8. (Color online) The zeroth-order radial $2p_{3/2}$ wave function (top) and the self-energy (SE) correction in Feynman gauge (bottom) for $Z = 92$. Units are the same as in Fig. 5.

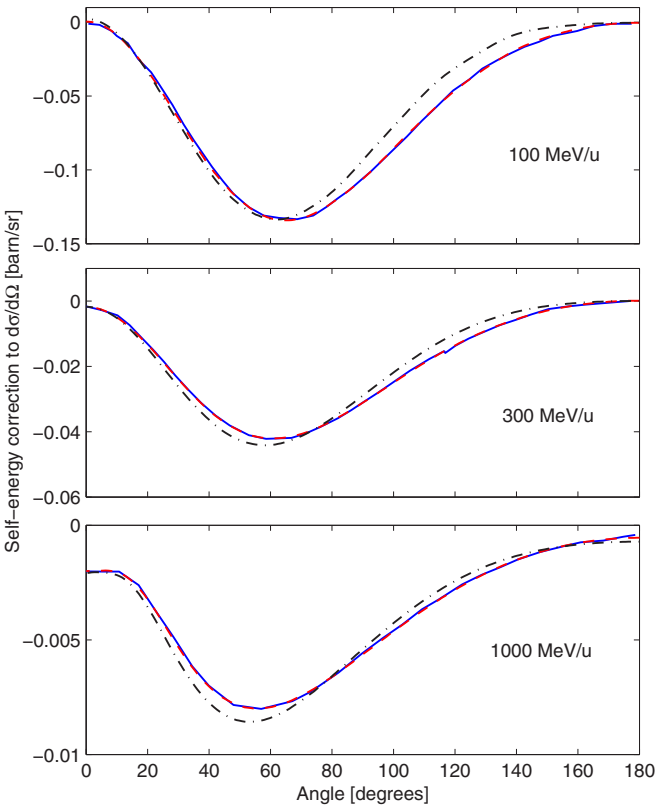

FIG. 9. (Color online) Self-energy wave-function and energy-shift corrections to the differential cross section of radiative recombination of an electron into the $1s$ state of bare uranium in the rest frame of the initial-state electron, for three different energies of the projectile (incoming bare uranium). The lines are: Feynman gauge (dashed red), Coulomb gauge (dash-dotted black), in comparison with the previous results by Shabaev *et al.* [8] (solid blue).

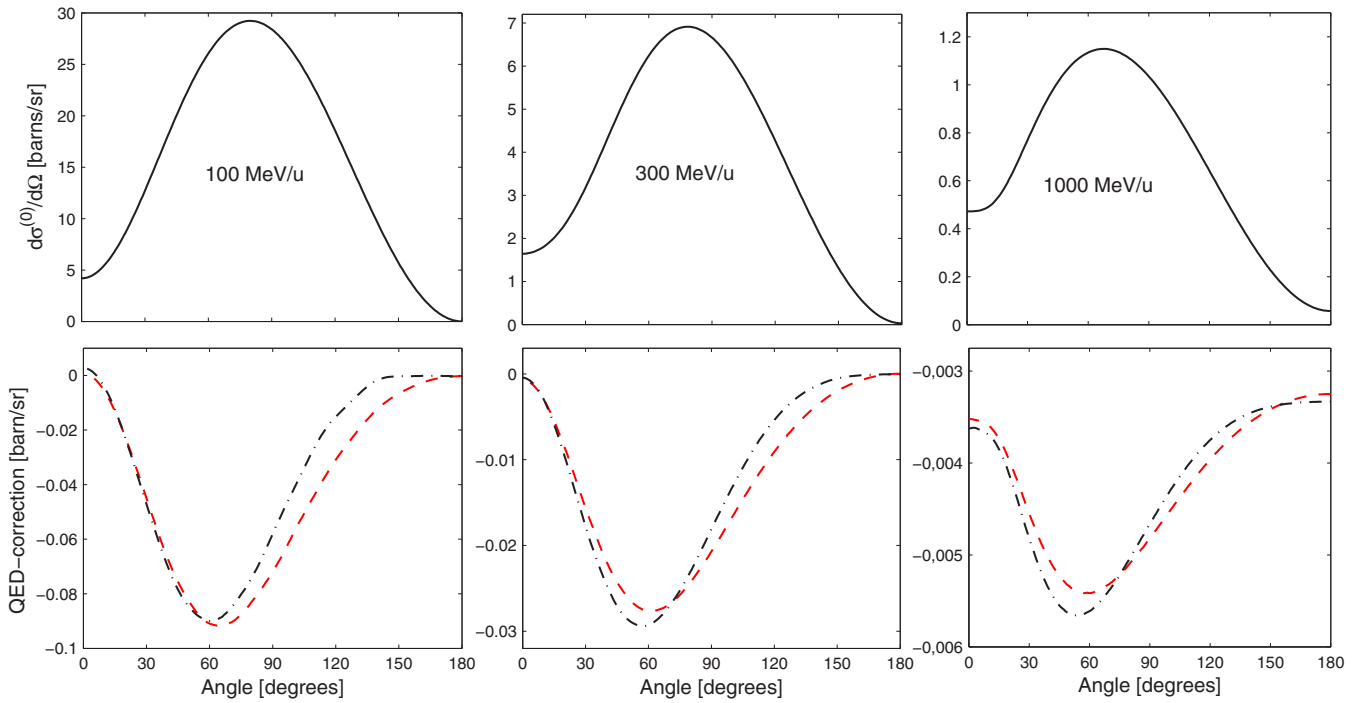

FIG. 10. (Color online) Differential cross section of radiative recombination of an electron into the $1s$ state of bare uranium in the rest frame of the continuum electron, for the ion-projectile energies 100 MeV/u, 300 MeV/u, and 1 GeV/u, respectively. Upper plots: zeroth-order cross section. Lower plots: the QED corrections (the self-energy and vacuum-polarization bound wave-function corrections and the correction due to the shift of the bound-state energy) in the Feynman gauge (dashed red line) and in the Coulomb gauge (dash-dotted black line).

gauge the bulk of the effect comes from the zero- and one-potential terms with the many-potential term acting as a relatively small correction. This can be advantageous in high-precision calculations since it is the many-potential term which typically sets the limit on the numerical accuracy of the final result, due to the extrapolations in terms of partial waves and grid size involved in its evaluation.

In Fig. 8 we show the Feynman-gauge self-energy correction to the $2p_{3/2}$ radial wave function in hydrogenlike uranium. Again, we see that the self-energy correction shifts the wave function outward in accordance with the positive energy shift. The typical size of the correction is one order of magnitude smaller than that for the $1s$ state (Fig. 5). This reflects the fact that the probability to find the $2p$-state electron in the nuclear region (where QED effects are most prominent) is much smaller than for the $1s$-state electron.

We proceed now to presenting applications of the radiatively corrected wave functions to calculations of QED corrections to radiative recombination and radiative decay.

B. *K*-shell radiative recombination

Figure 9 shows our Feynman- and Coulomb-gauge results for the self-energy correction to the differential cross section for radiative recombination of an electron into the $1s$ state of an initially bare uranium nucleus. The results are given in the rest frame of the initial electron, i.e., the laboratory frame where the incoming energetic bare nucleus captures a (quasi-free) electron from a stationary target. Good agreement is observed with the results from Ref. [8] obtained in Feynman gauge.

In Fig. 10 we plot the sum of the QED corrections computed in this work to the differential cross section. In contrast to Ref. [8], we did not include any corrections associated with a finite energy distribution of the initial continuum electrons. Thus, our results correspond to the scenario in which the energy spread of the continuum electrons is much smaller than the energy resolution of the photon detection. Our results are also not fully gauge invariant since we do not include the complete set of QED corrections of first order in α.

The corrections we have computed here behave qualitatively in the same way in both gauges and the difference between them is relatively small. One should not, however, interpret this as an indication that the uncalculated QED effects are small, as they may happen to be also similar in the two gauges. The obtained plots suggest that the relative size of the QED effects to the differential cross section grows with increasing energy (albeit quite slowly) and that these effects are most pronounced at a photon observation angle of roughly 60 deg.

In Fig. 11 we plot the polarization of the emitted radiation (the Stokes parameter P_1) as a function of observation angle, together with the QED correction δP_1 [Eq. (34)]. The results presented in these plots illustrate the energy dependence of the QED correction. In all three cases we observe that the maximum of the curve is shifted toward smaller angles; the size of the shift increases with the increase of the energy. The largest QED correction, however, appears in the lowest of the three projectile energies and in the very forward direction, at an angle of just 1 degree (see inset in the lower leftmost plot in Fig. 11).

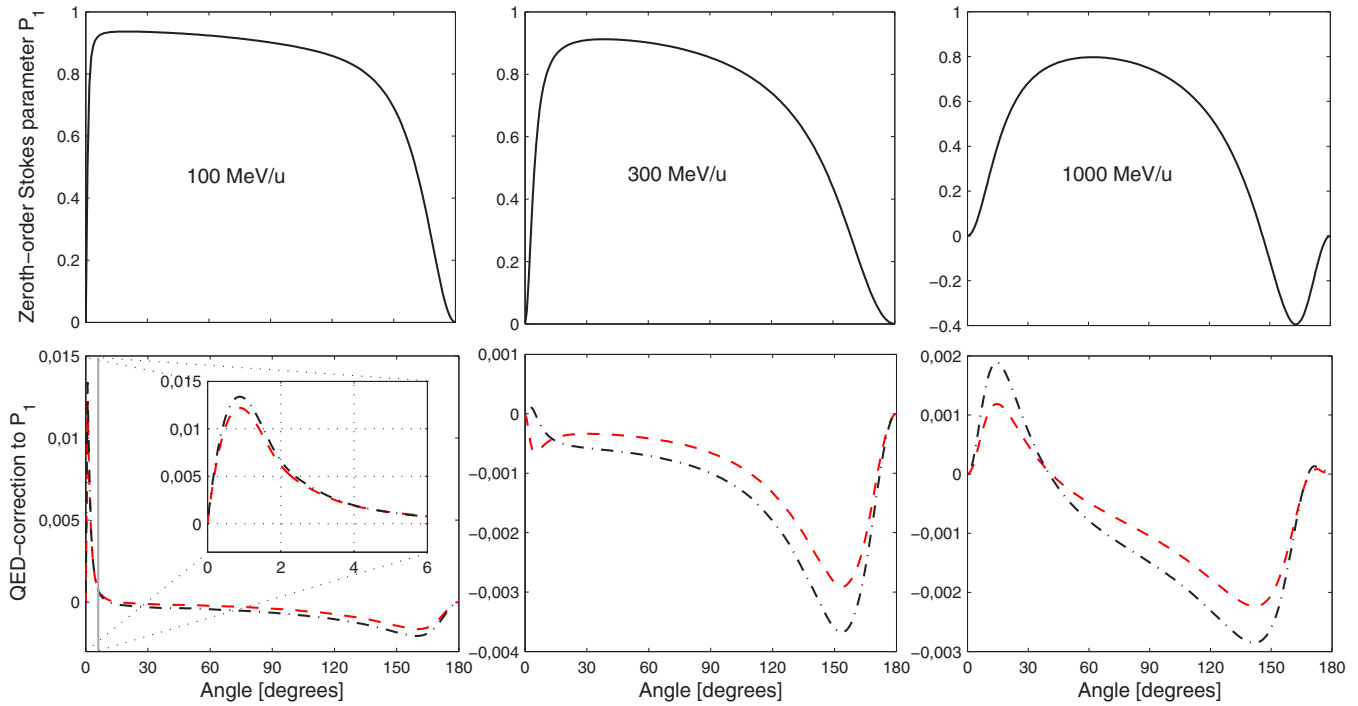

FIG. 11. (Color online) Polarization of the emitted radiation in the radiative recombination of an electron into the $1s$ state of bare uranium in the rest frame of the continuum electron, for the ion-projectile energies 100 MeV/u, 300 MeV/u, and 1 GeV/u, respectively. Upper plots: Stokes parameter P_1 in the zeroth-order approximation. Lower plots: the QED corrections (the self-energy and vacuum-polarization bound wave-function corrections and the correction due to the shift of the bound-state energy) in the Feynman gauge (dashed red line) and in the Coulomb gauge (dash-dotted black line). In the plot for 100 MeV/u we have inserted a zoom-in of the narrow region around the 1-degree direction.

C. Radiative decay

In Table I we present numerical values of the $E1$ and $M2$ reduced matrix elements for the $2p_{3/2} \to 1s$ transition in hydrogenlike uranium, as well as the ratio of the corresponding transition amplitudes τ_{M2}/τ_{E1}. The first row displays the results obtained with the point-nucleus Dirac energies and wave functions. The second row shows the corresponding results obtained with the extended nucleus. The next rows present the individual QED corrections and the final results. The calculation was performed in the Feynman gauge. The vacuum-polarization corrections include the Wichmann-Kroll contribution.

We found that the finite nuclear size and QED effects together induce the correction of -0.46% to the ratio of the $E1$ and $M2$ amplitudes. This is by almost factor of 40 smaller than the experimental error [5]. While our present calculations of QED effects are not complete and we cannot make a quantitative prediction for the total shift, it seems unlikely that QED effects can influence the interpretation of the experimental results of Ref. [5].

TABLE I. Individual contributions to the electric dipole and magnetic quadrupole reduced matrix elements and for the ratio of the corresponding transition amplitudes, for the $2p_{3/2} \to 1s$ transition in U^{91+}, in atomic units. SE denotes the self-energy corrections calculated in the Feynman gauge, VP denotes the vacuum-polarization corrections (including the Wichmann-Kroll contribution). Note that the specified uncertainties represent only the numerical errors of the calculated contributions; the uncertainty due to missing QED effects is not included.

Contribution	$\langle a\|\|\boldsymbol{\alpha}\cdot\mathbf{A}_1(e)\|\|b\rangle$	$\langle a\|\|\boldsymbol{\alpha}\cdot\mathbf{A}_2(m)\|\|b\rangle$	τ_{M2}/τ_{E1}
Dirac (pointlike nucleus)	0.0740699(1)	0.0062527(1)	0.084416(1)
Dirac (finite nuclear size, $R_{\rm nuc} = 5.863$ fm)	0.0741350(2)	0.0062458(1)	
SE: $2p_{3/2}$ wave function correction	−0.0000293(1)	−0.000000815(1)	
SE: $1s$ wave function correction	0.00008898(1)	0.00002677(2)	
VP: $2p_{3/2}$ wave function correction	0.000001016(1)	0.0000000415(1)	
VP: $1s$ wave function correction	−0.00001272(1)	−0.000006495(2)	
VP+SE: correction from energy shift	0.000041106(1)	−0.000028075(1)	
Sum QED + nuclear size	0.0742241(3)	0.0062372(1)	0.084032(2)
Difference			−0.000384(3)

V. SUMMARY AND OUTLOOK

A numerical method for calculating electron self-energy corrections to bound-state wave functions has been implemented. The resulting wave functions have been applied to a partial calculation of the one-loop QED correction to the process of radiative recombination of an electron with a bare uranium nucleus, as well as the corresponding corrections to the $M2/E1$ amplitude ratio for radiative decay of the $2p_{3/2}$ state in hydrogenlike uranium.

For radiative recombination we found good agreement with the previously reported Feynman-gauge results for the differential cross section. In the present work we also computed the self-energy corrections in the Coulomb gauge. Although gauge invariance is not expected at this level, we found a relatively small difference between the gauges. The corresponding QED corrections to the angular distribution of polarization parameter of the emitted radiation P_1 was also studied in both gauges. We saw an indication that the QED corrections are largest in the backward and (especially for the lowest energy considered) very forward directions.

For the ratio of the $M2$ and $E1$ transition amplitudes, we found that the finite nuclear size and QED effects together amount to a shift of the ratio of -0.46%.

The results obtained indicate the expected order of magnitude of the QED effects in these processes. In order to make a quantitative prediction, however, a complete calculation of all one-loop QED corrections is needed. Further development of the work described here would necessarily focus on the evaluation of the uncalculated terms, especially the vertex correction and reducible self-energy correction.

ACKNOWLEDGMENTS

J.H. wishes to thank Ingvar Lindgren and Sten Salomonson for valuable discussions. This work is supported by the Helmholtz Association and GSI under the project VH-NG-421. V.A.Y. acknowledges support by the Russian Federation program for organizing and carrying out scientific investigations.

[1] J. Eichler and T. Stöhlker, Phys. Rep. **439**, 1 (2007).
[2] T. Stöhlker, D. Banaś, H. Bräuning, S. Fritzsche, S. Geyer, A. Gumberidze, S. Hagmann, S. Hess, C. Kozhuharov, A. Kumar, R. Märtin, B. E. O'Rourke, R. Reuschl, U. Spillmann, A. Surzhykov, S. Tashenov, S. Trotsenko, G. Weber, and D. F. Winters, Eur. Phys. J. Special Topics **169**, 5 (2009).
[3] R. Reuschl, A. Gumberidze, T. Stöhlker, C. Kozhuharov, J. Rzadkiewicz, U. Spillmann, S. Tashenov, S. Fritzsche, and A. Surzhykov, Rad. Phys. Chem. **75**, 1740 (2006).
[4] S. Tashenov, D. Banaś, H. Beyer, C. Brandau, S. Fritzsche, A. Gumberidze, S. Hagmann, P.-M. Hillenbrand, H. Jörg, I. Kojouharov, C. Kozhuharov, M. Lestinsky, Y. A. Litvinov, A. V. Maiorova, H. Schaffner, V. M. Shabaev, U. Spillmann, T. Stöhlker, A. Surzhykov, and S. Trotsenko, Phys. Rev. Lett. **113**, 113001 (2014).
[5] G. Weber, H. Bräuning, A. Surzhykov, C. Brandau, S. Fritzsche, S. Geyer, S. Hagmann, S. Hess, C. Kozhuharov, R. Märtin, N. Petridis, R. Reuschl, U. Spillmann, S. Trotsenko, D. F. A. Winters, and Th. Stöhlker, Phys. Rev. Lett **105**, 243002 (2010).
[6] G. Weber, H. Bräuning, A. Surzhykov, C. Brandau, S. Fritzsche, S. Geyer, R. E. Grisenti, S. Hagmann, S. Hann, R. Hess, S. Hess, C. Kozhuharov, M. Kühne, R. Märtin, N. Petridis, U. Spillmann, S. Trotsenko, D. Winters, and T. Stöhlker, J. Phys. B **48**, 144031 (2015).
[7] V. M. Shabaev, Phys. Rev. A **50**, 4521 (1994).
[8] V. M. Shabaev, V. A. Yerokhin, T. Beier, and J. Eichler, Phys. Rev. A **61**, 052112 (2000).
[9] J. Sapirstein, K. Pachucki, and K. T. Cheng, Phys. Rev. A **69**, 022113 (2004).
[10] A. V. Volotka, D. A. Glazov, G. Plunien, V. M. Shabaev, and I. I. Tupitsyn, Eur. Phys. J. D **38**, 293 (2006).
[11] I. Lindgren, *Relativistic Many-Body Theory: A New Field-Theoretical Approach* (Springer, New York, 2011).
[12] I. Lindgren, S. Salomonson, and D. Hedendahl, Phys. Rev. A **73**, 062502 (2006).
[13] I. Lindgren, S. Salomonson, and D. Hedendahl, J. At. Mol. Opt. Phys. **2011**, 723574 (2011).
[14] J. Holmberg, S. Salomonson, and I. Lindgren, Phys. Rev. A **92**, 012509 (2015).
[15] D. Hedendahl and J. Holmberg, Phys. Rev. A **85**, 012514 (2012).
[16] L. W. Fullerton and J. G. A. Rinker, Phys. Rev. A **13**, 1283 (1976).
[17] P. J. Mohr, G. Plunien, and G. Soff, Phys. Rep. **293**, 227 (1998).
[18] P. J. Mohr, Ann. Phys. (NY) **88**, 26 (1974).
[19] P. J. Mohr, Ann. Phys. (NY) **88**, 52 (1974).
[20] S. A. Blundell and N. J. Snyderman, Phys. Rev. A **44**, R1427 (1991).
[21] P. Indelicato and P. J. Mohr, Phys. Rev. A **46**, 172 (1992).
[22] I. Lindgren, H. Persson, S. Salomonson, and A. Ynnerman, Phys. Rev. A **47**, R4555 (1993).
[23] H. H. Quiney and I. P. Grant, Phys. Scr. **T46**, 132 (1993).
[24] K. T. Cheng, W. R. Johnson, and J. Sapirstein, Phys. Rev. A **47**, 1817 (1993).
[25] V. A. Yerokhin and V. M. Shabaev, Phys. Rev. A **60**, 800 (1999).
[26] V. A. Yerokhin, K. Pachucki, and V. M. Shabaev, Phys. Rev. A **72**, 042502 (2005).
[27] G. E. Brown, J. S. Langer, and G. W. Schaeffer, Proc. R. Soc. London Sect. A **251**, 92 (1959).
[28] S. Salomonson and P. Öster, Phys. Rev. A **40**, 5548 (1989).
[29] S. Salomonson and P. Öster, Phys. Rev. A **40**, 5559 (1989).
[30] N. J. Snyderman, Ann. Phys. (NY) **211**, 43 (1991).
[31] G. S. Adkins, Phys. Rev. D **27**, 1814 (1983).
[32] G. S. Adkins, Phys. Rev. D **34**, 2489 (1986).
[33] A. Surzhykov, S. Fritzsche, T. Stöhlker, and S. Tachenov, Phys. Rev. A **68**, 022710 (2003).
[34] I. Lindgren, S. Salomonson, and J. Holmberg, Phys. Rev. A **89**, 062504 (2014).
[35] A. G. Fainshtein, N. L. Manakov, and A. A. Nekipelov, J. Phys. B **23**, 559 (1990).
[36] M. E. Rose, *Multipole Fields* (Wiley, New York, 1955).